Boon and Bane of 60 GHz Networks: Practical Insights into Beamforming, Interference, and Frame Level Operation

Thomas Nitsche, Guillermo Bielsa, and Irene Tejado
IMDEA Networks Institute and Universidad Carlos III, Madrid, Spain
{firstname.lastname}@imdea.org

Adrian Loch and Joerg Widmer
IMDEA Networks Institute
Madrid, Spain
{firstname.lastname}@imdea.org

ABSTRACT

The performance of current consumer-grade devices for 60 GHz wireless networks is limited. While such networks promise both high data rates and uncomplicated spatial reuse, we find that commercially available devices based on the WiHD and WiGig standards may suffer from their cost-effective design. Very similar mechanisms are used in upcoming devices based on the IEEE 802.11ad standard. Hence, understanding them well is crucial to improve the efficiency and performance of next generation millimeter wave networks. In this paper, we present the first in-depth beamforming, interference, and frame level protocol analysis of off-the-shelf millimeter wave systems with phased antenna arrays. We focus on (a) the interference due to the lack of directionality of consumer-grade antennas, and (b) the degree of data aggregation of current devices. Regarding (a), our beam pattern measurements show strong side lobes that challenge the common conception of high spatial reuse in 60 GHz networks. We also show that reflections in realistic settings worsen this effect. Further, we measure weak directionality when beamforming towards the boundary of the transmission area of an antenna array. Regarding (b), we observe that devices only aggregate data if connections require high bandwidth, thus increasing medium usage time otherwise.

CCS Concepts

•**Networks** → **Network experimentation;** *Physical links; Wireless local area networks;*

CoNEXT '15, December 01 - 04, 2015, Heidelberg, Germany

 ISBN 978-1-4503-3412-9/15/12…$15.00

DOI: 10.1145/2716281.2836102

Keywords

802.11ad; 60 GHz networks; practical performance; beamforming; interference; frame level protocol analysis

1. INTRODUCTION

Developing robust consumer-grade devices for millimeter wave wireless networks is challenging. In contrast to 802.11n/ac networks operating in the traditional 2.4 and 5 GHz ranges, devices based on the recent 802.11ad standard [1] for operation in the unlicensed 60 GHz range must overcome significant hurdles. This includes handling 2.16 GHz wide channels, using directional beamforming antennas to overcome the increased attenuation at these frequencies, and dealing with a highly dynamic radio environment [2, 3]. Existing work studies the *individual factors* that such a system must address regarding both the characteristics of 60 GHz communication—fading [4], reflections [5], frequency selectivity [6], and multipath effects [7, 8]—as well as the design of hardware such as phased antenna arrays [9–12]. The challenge is that consumer-grade devices must be able to handle the resulting complexity of the *overall system* while still being cost-effective.

This challenge has naturally led to the use of cost effective components in consumer-grade 60 GHz systems. For instance, current devices use electronic beam steering with relatively low order antenna arrays, that is, with only a limited number of active antenna elements. As a result, while the transmitters use directional beam patterns, they do not fully achieve the 60 GHz vision of extreme pencil-beam focusing and imperceptible interference impact. While this is *qualitatively* well-known, it raises a crucial question: how large is the practical, *quantitative* impact of such limitations?

Understanding this impact is fundamental since the aforementioned limitations may undermine common 60 GHz assumptions. This in turn is key to design protocols that can reliably operate on millimeter wave frequencies. As a quantitative analysis of these limitations is missing, the following issues remain unanswered:

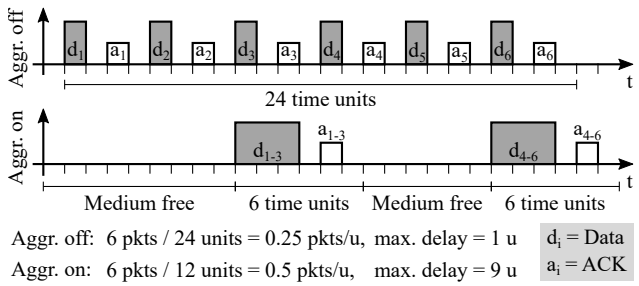

Figure 1: Aggregation primer. In general, it increases throughput and reduces medium usage, but worsens delay. It's impact is particularly large in 60 GHz due to the very high data rates.

A. **Directional communication.** How directional are consumer-grade phased antenna arrays? How large is the actual impact of side lobes?

B. **High spatial reuse.** How close can devices operate without experiencing collisions? How strong is the impact of interfering reflections?

C. **High data rates.** Which coding and modulation schemes are feasible? What is the impact of data aggregation *at such data rates* (c.f. Figure 1)?

Previous work using consumer-grade 60 GHz devices is limited to studying the impact of human blockage [13] and transmission range [14]. In this paper, we provide answers to the questions above. To this end, we use a down-converter to overhear and analyze the communication of 60 GHz devices. This gives us unprecedented insights into link utilization[1], beam patterns, and frame level operation, since the existing devices themselves do not provide any of this information. This analysis allows us to determine the key limitations of 60 GHz consumer-grade hardware, which opens the door to future work on mechanisms that address these limitations. In particular, our contributions are as follows:

1. We provide a frame level analysis of WiGig, studying its frame length and showing that WiGig only uses data aggregation if a connection requires high throughput. Otherwise, it does not aggregate, even for traffic that is not necessarily delay-constrained.

2. We measure the beam patterns that our devices use. We show that quasi omni-directional antenna patterns suffer significant imperfections. Further, directional beam patterns exhibit very strong side lobes of up to -1 dB compared to the main lobe.

3. We evaluate the impact of interference due to side lobes. We observe a perceptible impact for distances of up to five meters. We show that this effect worsens at the boundary of an antenna array's transmission area due to increased side lobes.

4. We study the impact of reflections in realistic wireless settings. We find that interfering reflections from neighboring, unaligned devices may reduce the achievable TCP throughput by more than 20% of the value that would be achieved otherwise.

[1]We use *link utilization*/*medium usage* interchangeably.

The paper is structured as follows. Section 2 gives an overview on millimeter wave communication. Section 3 provides details on the tested devices and our measurement setup. In Section 4, we present the details of our measurement campaign, and in Section 5 we discuss the results. Finally, Section 6 concludes the paper.

2. BACKGROUND

In this section, we describe the characteristics of millimeter wave communications, and present related work in this area. Millimeter wave frequencies have been used for commercial wireless systems for several years. These first generation systems, however, were targeting mainly static or pseudo static application scenarios, like backhaul links (for example the HXI Gigalink 6451 system used in [14]) or transmission of uncompressed high definition video data [13]. With formation of the WiGig Alliance [15], the latter use case broadened to docking station applications and finally incorporated general WiFi use cases when, in 2012, WiGig was merged into the IEEE 802.11ad amendment. This amendment defines a unified millimeter wave communication standard for a variety of use cases, that include dense deployment scenarios with (limited) mobility [2].

Transmission Characteristics. Communication in the millimeter wave range has distinctly different communication characteristics than those of legacy ISM frequencies below 6 GHz. These differences mainly result from the increased attenuation of free space propagation and signal blockage in case of obstacles [16]. The increased attenuation of around 20-40 dB is typically overcome by highly directional antennas. These may also be used to circumvent blockage, using a propagation path via a first order reflection that certain highly reflective materials provide [5]. Further, directional communication and blockage significantly lower the amount on interference on millimeter wave frequencies and allow for high levels of spatial reuse.

Beam Steering. With the central role of directional communication in millimeter wave systems, a device's ability to steer its directional beams becomes essential. As the size of antennas scales with the wave length, millimeter wave systems can integrate antenna arrays with a high number of elements even into small handheld devices. Theses antenna arrays allow electronic configuration of the antennas' beam direction and provide very high directional gain. In contrast to lower frequency beamforming mechanisms, millimeter wave systems usually rely on beam steering via codebooks of predefined beam patterns that implement different directions, which reduces the complexity of transceivers and of the beam training process. While such millime-

ter wave antenna arrays have been in use since first generation devices, little is known about their impact on system level network performance.

Work on Practical 60 GHz Networks. Insights into practical 60 GHz *networks* are limited since 802.11ad hardware is not available yet. However, related work uses WiGig and WiHD devices to study study the performance of 60 GHz links, similarly to this paper. For instance, Zheng et al. [14] uses off-the-shelf hardware to characterize 60 GHz links, dispelling a number of common beliefs regarding millimeter wave communication. This includes showing that the range of such networks is large enough for outdoor communication, and that electronically steerable antenna arrays can deal with blockage as well as user motion. Still, in contrast to our work, they do not study and measure the antenna patterns of off-the-shelf hardware to investigate interference in 60 GHz networks. Further, they focus on high-level metrics of 60 GHz links such as throughput, while we analyze the frame level operation of WiGig to study the impact of data aggregation in 60 GHz networks.

Ramanathan et al. [17] follow a different approach than [14] and, hence, us. Instead of measuring the performance of off-the-shelf devices, they use a custom-built software-defined radio that allows them to perform signal strength measurements at 60 GHz using horn antennas. Among other results, they show that different types of link breaks should be treated differently. For instance, a transmitter should change beam direction to avoid human blockage, whereas it should widen its beam to deal with mobility. Most interestingly, they show how the signal strength can be used for early detection of each type of link break. In contrast, we study actual data transmissions using hardware with electronically steerable phased antenna arrays. While [17] focuses on blockage, beam steering, and spatial reuse assuming horn antennas, we investigate topics such as reflections for range extension, data aggregation, and interference due to imperfections of commercial 60 GHz hardware.

3. MEASUREMENT SETUP

Next, we present the evaluated 60 GHz systems and the used measurement equipment. Further, we describe the setups for the frame level analysis, as well as the beamforming, reflection and interference measurements.

3.1 Devices and Measurement Equipment

We evaluate two different millimeter wave systems in order to analyze their behavior and performance in real-world settings and investigate inter-system interference. As of today, no off-the-shelf 60 GHz system allows access to any significant MAC or PHY level informations. Hence, we use a 60 GHz down-converter together with an oscilloscope to overhear the communication.

Devices Under Test. Our first device under test is the Dell D5000 wireless docking station, which follows the WiGig standard. The docking station allows connections by Dell notebooks with a compatible WiGig card and antenna module. We use Latitude E7440 notebooks as remote stations. The system can connect multiple USB3 devices using the wireless bus extension (WBE) protocol, as well as multiple monitors. The serviced area with best reception is in a cone of 120 degree width in front of the docking station. In indoor environments, over short link distances, and with reflecting obstacles, we found it, however, to perform over a much wider angular range. The maximum achievable distance depends on the environment and fluctuates between 12 and 18 meters. During disassembly, we found that both docking station and notebook module are manufactured by Wilocity. Both sides consist of a baseband chip connected to an upconverter and a 2x8 element antenna array. The docking station comes with an application that provides limited configurability (e.g., channel selection) as well as PHY data rate readings.

Our second system is a WiHD-compatible DVDO Air-3c system for the transmission of HDMI data streams. The system has transmitter and receiver modules that do not allow for any configuration and do not provide link state information. When testing the transmission range and link stability, we found that it performs better than the D5000. Indoors, we could transmit video over 20 meters, even with 90 degree misalignment and blockage on the direct path. Upon disassembly, we found on both sides of the link a 24 element antenna array with irregular alignment in rectangular shape. The bandwidth of both the D5000 and the Air-3c is 1.7 GHz. They both operate on center frequencies 60.48 GHz and 62.64 GHz.

Measurement Equipment. To collect data for frame level analysis and received signal power measurements, we use a Vubiq 60 GHz development system in conjunction with an Agilent MSO-X 3034A oscilloscope. We use this setup to obtain traces of the analog I/Q output of the Vubiq receiver. In most experiments, we undersample the signal at 10^8 samples per second. While this prevents decoding, it allows us to extract the timing and amplitude of different frames by processing the traces offline in Matlab. The frontend supports downconversion of 1.8 GHz modulated bandwidth at the common IEEE 802.11ad/aj frequencies [18]. Further, it has a WR-15 wave guide connector which allows us to connect horn antennas with different levels of directivity. For beam pattern measurements, we use a 25 dBi gain horn antenna. To obtain a wide beam pattern for protocol analysis, we use the open wave guide.

3.2 Measurement Setup

In the following, we explain the setup of the four measurement studies that we present in this paper, namely, the analysis of the frame level protocol operation, beam patterns, interference, and reflections.

Frame Level Protocol Analysis. In order to gain insights into the protocol operation of the devices under test, we down-convert their signals to baseband and analyze them in Matlab. To this end, we use the wide

reception pattern of the open wave-guide of the Vubiq system. This allows us to overhear the frames of both the transmitter and the receiver.

For the Dell D5000 case, we use the laptop as the transmitter and the docking station as the receiver. To identify which frames come from which device, we place the Vubiq down-converter behind the docking station and point it towards the notebook's lid. As a result, the down-converter receives the frames of the notebook via a direct path, and the frames of the docking station via a reflection from the notebook's lid. Thus, the average amplitude of the notebook frames is larger than the one of the docking station frames, and we can easily separate them. We use Iperf[2] to generate TCP traffic on the WiGig link that connects the laptop with the Ethernet adapter at the docking station. We run the Iperf server on the laptop and the Iperf client on a second system connected via Ethernet to the docking station.

For the wireless HDMI case, we place the Vubiq down-converter close to the transmitter. No reflector setup is needed since the frames of the receiver inherently have a larger amplitude. Again, we post-process the collected signal traces in Matlab to analyze their structure. We carry out most of the trace analysis using automated algorithms. However, we also use manual inspection to draw some of our conclusions in Section 4.1.

Beam Pattern Analysis. To analyze the directivity and side lobes of the antenna patterns, we use the Vubiq system with a highly directional horn antenna as described in Section 3.1. By aligning this setup to the device under test, the impact of the second device in an active link is almost imperceptible, which allows for accurate beam pattern measurement. As beam patterns change once data transmission starts after link initialization, we also measure the patterns of trained links.

We measure the azimuthal plane of the beam patterns on a large outdoor space to avoid unwanted reflections. In particular, we capture signal energy on 100 equally spaced positions on a semicircle with radius 3.2 m. To this aim, we rotate the entire setup—i.e., the Vubiq and the oscilloscope—along all measurement locations, and collect signal traces at each position. Figure 2 shows our setup. We place the device under test in the center of the semicircle, and ensure a clear line of sight between transmitter and receiver throughout the experiment to prevent unwanted beam training. Due to the high directivity of the horn antenna that we use, we found that the most powerful data frames always belong to the device under test. When processing the traces, we ensure that we extract signal strength from data frames only. We discard periodic control frames, which are transmitted with higher power and wider antenna patterns. The signal strength in every location is then averaged over the filtered frames recorded over the span of one minute.

Further, we analyze the device discovery behavior of the Dell D5000 docking station. When disconnected,

[2]https://iperf.fr/, version 2.0.5-3

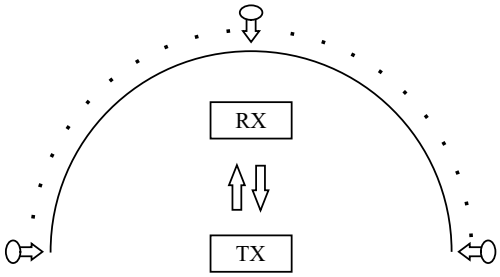

Figure 2: Beam pattern analysis setup.

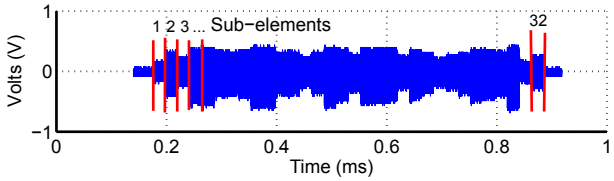

Figure 3: Dell D5000 device discovery frame.

the system frequently emits a device discovery frame that is transmitted over multiple antenna patterns to cover an area as large as possible. An example for this frame type is shown in Figure 3. It can be seen that the frame consists of 32 sub-elements, each with relatively constant amplitude. Each of these sub-elements is transmitted with a different antenna configuration. As the pattern sequence of the sub-elements is the same for all frames, we can measure them using the same averaging approach as for active data transmissions. We then split the frame into its sub-elements during post processing to find the beam pattern of each sub-element.

Reflection Analysis. Next, we analyze the impact of reflections in a realistic wireless setting. This addresses the common assumption that 60 GHz reflections are very limited compared to the 2.4/5 GHz case, and result from quasi-optical propagation in the direction of transmission. To this end, we set up a single 60 GHz link in an empty conference room, either using the D5000 or the WiHD system. We then measure the energy received from all possible directions at six different locations $\{A \dots F\}$ in the room, as shown in Figure 4. If no reflections occur, we expect to receive energy only from the direction in which the transmitter is located. For instance, at location A in Figure 4, we should only observe energy coming horizontally from the right. Additional lobes in the corresponding angular profile indicate reflections. To analyze the impact of different materials, we perform the experiments in a room which has brick, glass, and wood walls. Figure 4 shows the material layout. To measure the angular profile at each location, we mount the Vubiq receiver on a programmable rotation device and place it at each of the six locations in Figure 4. Moreover, we attach a highly directional horn antenna to the receiver. At each location, we then mea-

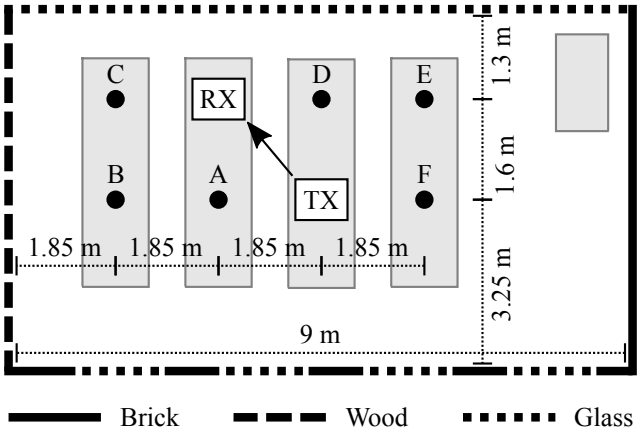

Figure 4: Reflection analysis setup.

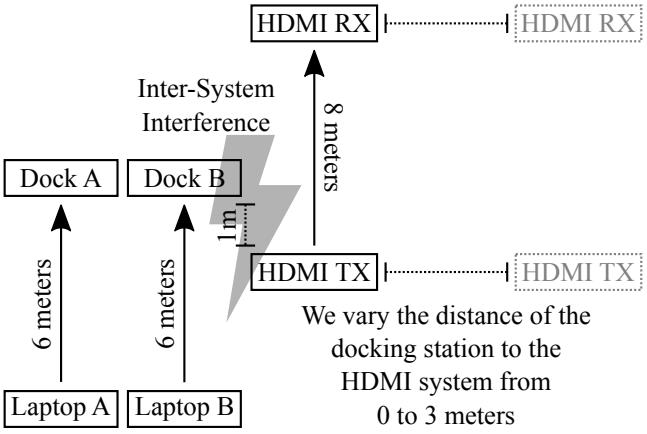

Figure 6: Interference analysis setup.

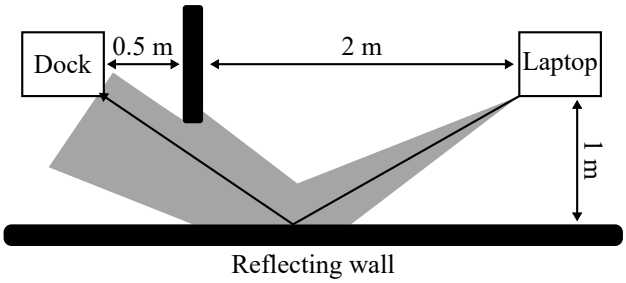

Figure 5: Reflection throughput setup.

sure the incident signal strength in each direction and assemble the result to an angular profile.

While the above setup allows us to show that reflections are significant, we also perform a case study to analyze whether those reflections may help to extend the coverage of a network if the line-of-sight is blocked. To this end, we set up a link parallel to a wall using a D5000 docking station and its corresponding laptop. Additionally, we place an obstacle in between both. We then measure the angular energy profile at the receiver to verify that the line-of-sight path is actually blocked, and that all energy arrives via the reflection off the wall. Finally, we use Iperf to measure the achievable rate on such a reflection. Figure 5 depicts our setup.

Interference Analysis. To analyze how interference affects 60 GHz communication, we operate multiple 60 GHz systems in parallel on the same channel. In particular, we use two pairs of notebooks connected to D5000 docking stations and the DVDO Air-3c WiHD system, as shown in Figure 6. The Dell D5000 systems do not interfere with each other since they use CSMA/CA to share the medium. However, we use two of them in parallel to increase wireless medium utilization, and thus raise the probability of observing interference with the WiHD system. The WiHD system does not use CSMA/CA and blindly transmits data causing collisions and retransmissions at the D5000 systems. That is, the inter-system interference in Figure 6 is due to the impact of the "HDMI TX" on "Dock A" and "Dock B". We set the distance between the WiHD transmitter and receiver to eight meters to ensure that the transmitter transmits frames with sufficiently high power. A scenario comparable to this setup could be caused for example by two close-by millimeter wave systems connected to different access points in a multi-AP network. Further, we vary the horizontal distance between the D5000 and the WiHD system in the range from 0 to 3 meters to analyze the impact of the interference incidence angle. As we found that the WiHD system transmits with a much wider antenna pattern than the D5000, this procedure creates interference whenever a side lobe of the D5000 system matches the interferes direction. To measure the effect of interference we measure link utilization, reported link rate and the time of transmission of a file with a size of 1 GB. To obtain link utilization measurements we collect seven minutes of channel traces and use a threshold based detection approach to calculate the ratio of idle channel time. While the formerly described reflection analysis allows us to assess the existence and strength of reflections, we use a second setup to determine the impact of those reflections on data transmissions. In particular, we set up two geometrically non-interfering 60 GHz links close to a metal reflector, as shown in Figure 7. To eliminate the influence of side lobes on the measurement, we position shielding elements close to the WiGig devices. Further, we make sure that we do not block the reflected signal resulting from the metallic surface behind the WiHD receiver. We then analyze the coverage area of this reflection using the Vubiq transceiver to ensure that the docking station is located inside. Finally, we perform a TCP throughput measurement, with frame flow from the laptop to the docking station. By powering on and off the WiHD devices, we can evaluate the impact of the reflected signal on the WiGig TCP connection.

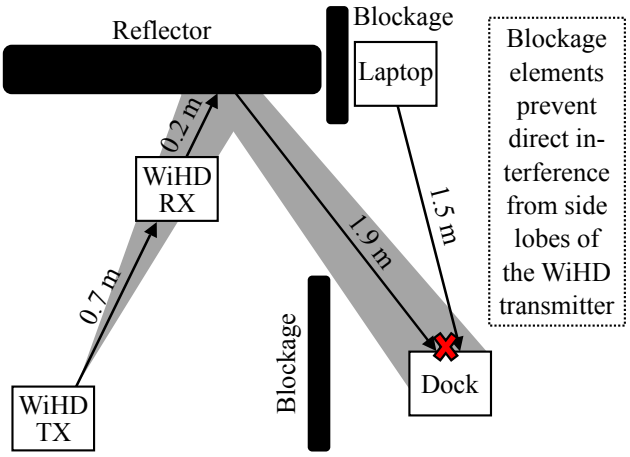

Figure 7: Reflection interference setup.

Frame type	Repeat interval
D5000 Device Discovery Frame	102.4 ms
D5000 Beacon Frame	1.1 ms
WiHD Device Discovery Frame	20 ms
WiHD Beacon Frame	0.224 ms

Table 1: D5000 and WiHD frame periodicity.

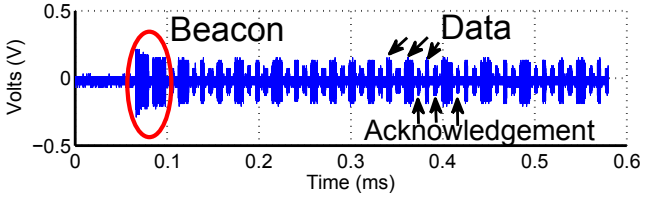

Figure 8: Dell D5000 frame flow.

4. RESULTS

In this section we present the results of our measurements using the setups described in Section 3. We first present our findings on protocol operation and data aggregation. Second, we analyze the beamforming capabilities of the D5000. Third, we investigate the impact of reflections. Finally, we evaluate the interference between WiGig and WiHD, including reflections.

4.1 Protocol Analysis

We study the flow of frames between the devices under test using the Vubiq receiver. In particular, we analyze the frame structure of both the D5000 and the WiHD system, as well as the frame length and the burst length of the D5000. The latter allows us to get insights into the impact of data aggregation.

Dell D5000. The Dell D5000 follows the WiGig standard. This is particularly interesting since the later versions of the standard are closely related to the IEEE 802.11ad standard. Hence, the behavior of existing consumer-grade WiGig devices reveals the issues that future devices based on IEEE 802.11ad will face. The WiGig protocol description is not freely available, but we observe that it consists of three phases, namely, device discovery, link setup, and data transmission. In the first stage, the docking station emits a characteristic device discovery frame that is transmitted over several quasi omni-directional beam patterns shown in Figure 3. The frequency of these beam sweep frames is given in Table 1. A detailed beam pattern analysis of this frame follows in Section 4.2. At the second stage, a complex association and beamforming process between dock and remote station takes place. Finally, when the link is set up completely, data transmission begins.

Our frame level analysis shows that the data transmission phase contains bursts, similarly to the IEEE 802.11ad EDCA transmit opportunities (TXOP). The maximum length of such bursts is 2 ms. Each burst begins with two control frames, which have a different amplitude than the subsequent series of data and acknowledgment frames, as shown in Figure 8. These control frames are most probably an RTS/CTS exchange, which is crucial due to the deafness effects resulting from the directional transmission. Outside the bursts, the channel is idle except for a regular beacon exchange between the docking station and the notebook. The transmission frequency of these beacons is given in Table 1.

To study data aggregation, we measure the length of data frames for different TCP throughput values. We control the TCP throughput by adjusting its window size in Iperf. Figure 9 depicts the CDF of the frame lengths for each throughput value. The CDF reveals that frames are either short (around 5 μs) or long (15 to 20 μs). That is, we can divide them into two categories. The length of long frames varies more than the length of short frames, which may be due to different levels of aggregation. The highest level we observed corresponds to a frame duration of 25 μs. Further, the amount of long frames *increases* with throughput—the higher the traffic load, the more data aggregation. This matches Figure 10, which shows the fraction of long frames, i.e., longer than ≈ 5 μs, for increasing throughput values.

Moreover, we investigate the level of medium usage for increasing throughput values. Surprisingly, Figure 11 shows that, beyond a relatively low throughput value[3], all oscilloscope traces contained data frames. That is, the transmitter transmitted *continuously*. Hence, the throughput increase is not due to a higher medium usage but could be either due to a higher modulation and coding scheme (MCS), or a higher level of data aggregation. Figure 12 answers this question—it depicts the raw physical layer data rate reported by the D5000 over a timespan of ten minutes. For short links, Figure 12

[3]We choose values in the order of *kilobits* per second to observe low link utilization. We achieve these values by setting a small TCP window size (≈ 1 KB) in Iperf.

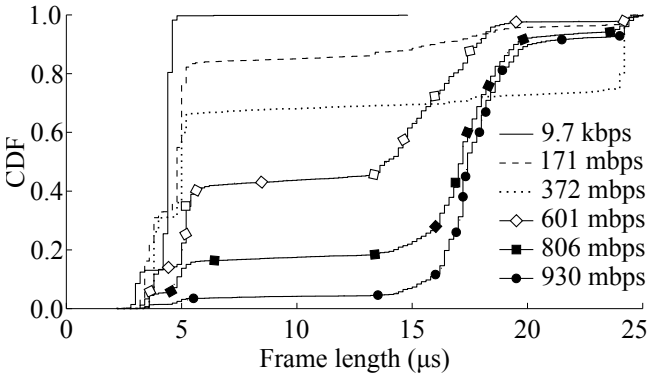

Figure 9: WiGig data frame length.

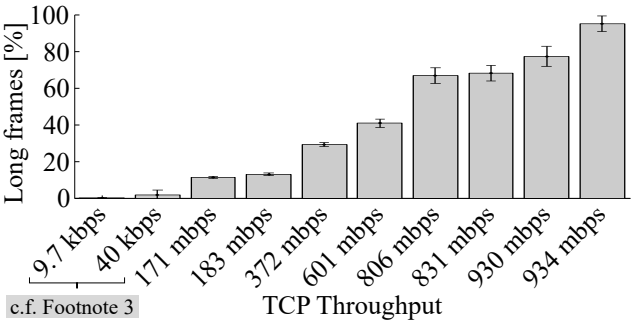

Figure 10: Percentage of long frames in WiGig.

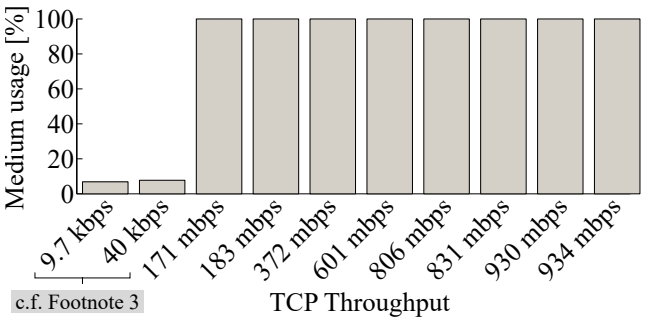

Figure 11: WiGig medium usage.

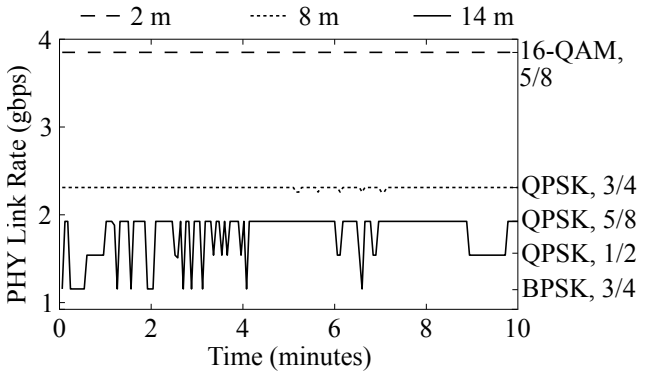

Figure 12: MCS with low traffic.

shows that WiGig uses a very high MCS. This explains the low link usage for 9.7 and 40 kbps in Figure 11, which were also measured at a short distance. Further, it suggests that the MCS is not adapted to the link load, as expected. Hence, we conclude that high throughput values are achieved exclusively by means of data aggregation, as the MCS naturally only depends on the signal strength. That is, for a constant MCS and medium usage, WiGig can scale throughput from 171 mbps to 934 mbps by aggregating only 25 μs of data, which is 320× less than what 802.11ac needs for just a 2× gain [19].

Figure 12 also shows the impact of the link length on the physical layer rate. As expected, the longer the link, the lower and unstable the data rate. While Figure 12 depicts the link rate, in Figure 13 we show the average Iperf throughput at increasing distances. We observe that link rate is approximately stable up to a certain distance d and then falls abruptly. This distance d varies significantly for different experiments, ranging from 10 to 17 meters. As a result, while the individual experiments clearly exhibit the aforementioned abrupt behavior, the average falls gradually. From Figures 12 and 13 we conclude that the MCS drops gradually with distance to about 1 gbps but then falls abruptly. In Figure 13 we do not observe results beyond roughly 900 mbps because the Gigabit Ethernet interface at the docking station limits the achievable throughput.

Unless indicated otherwise, we carry out all of our experiments for links below two meters. Interestingly, the rate reported by the WiGig driver matches the MCS levels defined in the standard for single-carrier mode [15], which suggests a direct relation. Figure 12 includes the MCS that corresponds to each of the rates we measure. While we reach 16-QAM with 5/8 coding—the second highest MCS in the standard—we never observed the highest MCS. We measure the rates in Figure 12 in a stable environment without mobility. Naturally, our results are mostly constant for short link lengths. Still, Figure 12 only shows a relatively short time interval. Figure 14 depicts the rate and amplitude under similar conditions for roughly one hour. In this case, we observe that the link rate varies occasionally. Moreover, this occurs precisely when the signal amplitude changes[4]. Since the environment is constant, such amplitude variations are most probably due to a beam pattern realignment. This suggests that rate adaptation and beam pattern selection are implemented as a joint process in the Dell D5000 system.

[4]In Figure 14, the bit rate decreases when the amplitude increases. This counterintuitive behavior is because we measure the bit rate at the D5000 and the amplitude at the Vubiq receiver. Due to the directivity of the signal, a decrease at the Vubiq does not necessarily mean that the signal also has less amplitude at the D5000.

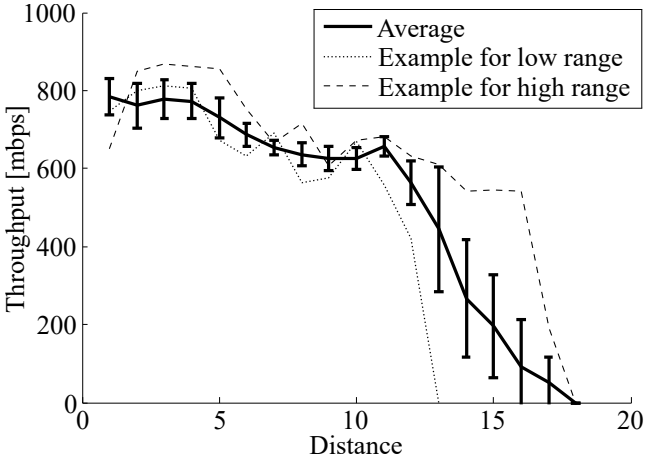

Figure 13: Throughput decrease with distance.

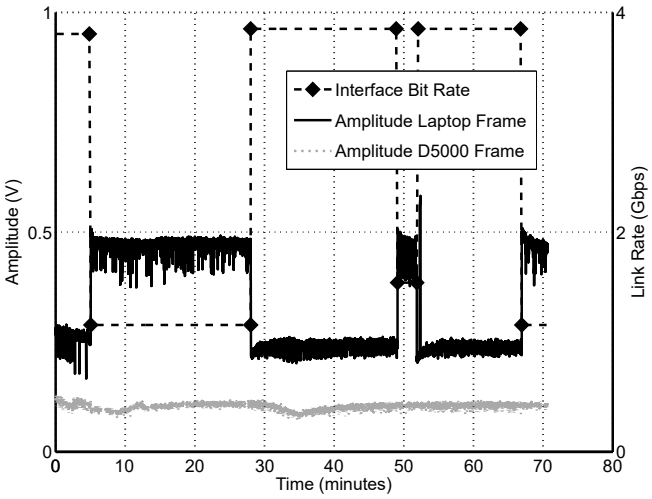

Figure 14: D5000 frame amplitudes and rate.

DVDO Air-3c. Next, we analyze the frame flow for the DVDO Air-3c WiHD system. We observe the same communication stages as for the Dell D5000 system. The frequency of device discovery frames transmitted by the WiHD devices is given in Table 1. When analyzing the data transmission stage, we found the beacon frame frequency to be much higher than for the D5000 system. Also the data transmission process significantly differs. Figure 15 shows an example frame flow for the WiHD system. In contrast to the D5000, there is no clear data/acknowledgement frame exchange. Instead, the transmitting device emits data frames of variable length following periodic beacons of the receiver. Whenever no data is queued for transmission, we only observe beacon frames. The trace shows the transition from an active video data transmission period to an idle period. The WiHD system does not seem to perform channel sensing, which has a significant impact regarding interference (c.f. Sections 4.3 and 4.4).

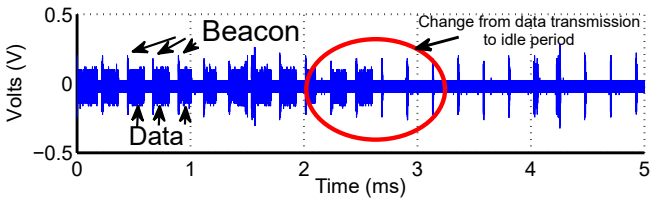

Figure 15: DVDO Air-3c WiHD frame flow.

Our results show that data aggregation is key for 60 *GHz communication. In particular, we observe that aggregation improves throughput from* 170 *mbps to* 930 *mbps, i.e., a* 5.4× *gain. Our measurements also suggest that, for distances beyond* 10 *m, links become unstable and often break before the transmitter switches to rates below* 1 *gbps. Finally, link rates may fluctuate even in static scenarios due to beam pattern realignments.*

4.2 Beam Patterns

Next, we measure the antenna patterns of the D5000. We first investigate the quasi omni-directional patterns used for device discovery. After that, we analyze the highly directional patterns used for data transmission.

Quasi Omni-directional Search. Implementation of omni-directional antenna patterns is a major challenge for millimeter wave communication [9]. However, this kind of pattern is needed for device discovery and beam training [2]. The Dell D5000 system sweeps 32 different quasi omni-directional patterns during its remote station search before the link setup. Each of these patterns is used during a sub-element of the device discovery frame. The device discovery frame is continuously repeated by the D5000 until a connection is established.

Figure 16 shows four out of the 32 different antenna patterns that the D5000 sweeps during link establishment. The irregularities of the beam patterns are a natural result of our measurement setup—since we manually move the Vubiq receiver along the 100 measurement positions (c.f. Section 3.2), small deviations are inevitable. Nevertheless, Figure 16 clearly depicts the rough shape of the lobes. While the half power beam width (HPBW) can be as wide as 60 degrees, each pattern contains several deep gaps that may prevent communication with devices at this specific angle. These gaps are due to the limitations of consumer-grade phased antenna arrays. The remaining 28 patterns are comparable in terms of directional focus and received signal power. The device discovery frame of the WiHD system also sweeps several quasi omni-directional beam patterns. However, their order changes with every transmitted device discovery frame. Hence, measuring the beam patterns with our setup is not practicable.

Device discovery in 60 GHz systems proves to be a challenging process. We find that the two systems that we test repeatedly sweep multiple quasi omni-directional beam patterns to reliable reach a pairing device. In particular, one of the systems sweeps 32 different patterns.

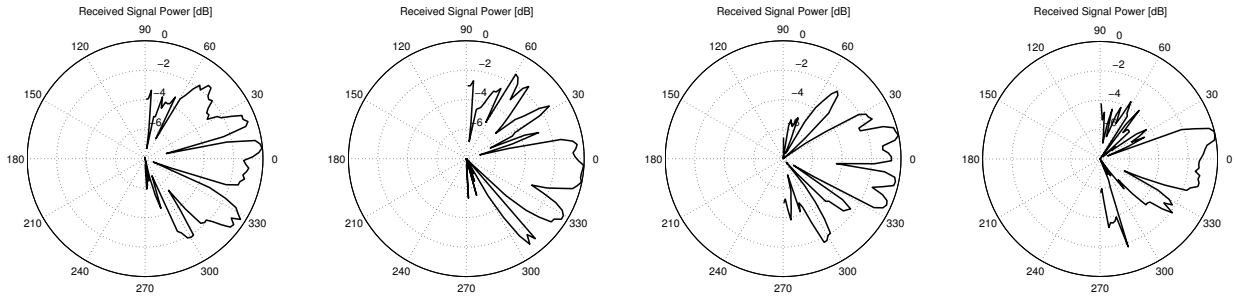

Figure 16: Quasi omni-directional beam patterns swept by the D5000.

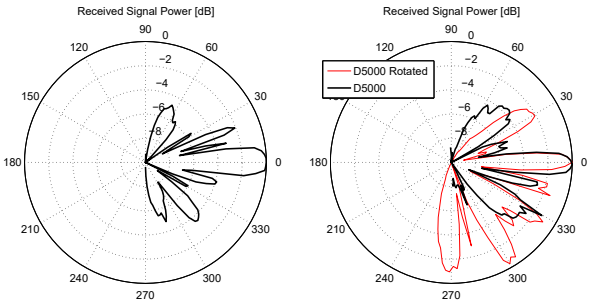

Figure 17: Laptop (left) and D5000 (right) beam patterns. Main lobe points always to 0 degrees.

Directional Transmission and Side Lobes. Next we evaluate the beam pattern used by the D5000 system during the data transmission stage. There, in contrast to the device discovery frames during the link setup, highly directional antenna configurations are used. Figure 17 shows the measured transmit patterns of a Dell E7440 notebook and the D5000 docking station. The patterns are of highly directional nature with a HPBW below 20 degree. Despite the strong signal focus, significant signal energy is measured from side lobes. These side lobes can have a transmit power in the range of -4 to -6 dB compared to the main lobe, and thus can cause major interference effects. The asymmetry of the pattern—especially for the notebook—results from the antenna being placed at the side of the notebook's lid.

In a second measurement we introduce a misalignment of 70 degrees between docking station and notebook. Figure 17 shows the resulting docking station beam pattern as an overlay. While measuring this pattern, we had to increase the receiver gain by 10 dB. That is, beamforming towards the boundary transmission area of the antenna array significantly reduces link gain. Also, we observe a much higher number of side lobes as strong as -1 dB with respect to the main lobe.

While antennas are already highly directional, strong side lobes exist. Further, the placement of the antenna inside a device has a noticeable impact on the antenna pattern. When beamforming close to the outer limit of an array's transmission area, directionality is reduced and the number of strong side lobes increases.

4.3 Reflections

In the following, we present our reflection results for the setup shown in Figure 4. Figures 18 and 19 depict the angular profiles that we measure for the D5000 and the WiHD system, respectively. In both cases, most angular patterns have at least two clearly identifiable lobes—one pointing to the transmitter and one pointing to the receiver. The reason for the latter is that the receiver not only receives data frames but also transmits the corresponding acknowledgments. However, a significant number of angular patterns feature additional lobes that do not point to any of the devices in the room. This is a clear indication of reflections off the walls. In contrast to common assumptions regarding 60 GHz communications, the lobes show a significant amount of incidence energy. For instance, the angular pattern at position F in Figure 18 has a lobe directly pointing to the lower wall. Geometrically following the reflection of the signal off the nearby window suggests that this lobe is due to the transmitter. Further, the angular pattern at position B features a lobe pointing towards the wooden wall. However, this lobe can only arise from a *second order* reflection originating at the receiver, and bouncing off both the glass wall as well as the wooden wall. In comparison to the D5000, the WiHD system shows similar effects. However, the angular patterns in Figure 19 feature more and larger lobes than in Figure 18. This suggests that the WiHD system is less directional than the D5000, and thus produces significantly more reflections. As a result, the impact on spatial reuse is even higher. This matches earlier observations throughout our measurement campaign. In Section 4.4, we analyze this effect in detail.

Reflections are strong and may thus undermine the alleged spatial reuse of 60 *Ghz systems. Moreover, second order reflections occur and may have a large impact.*

Additionally, we study whether reflections may help to extend the range of 60 GHz links beyond obstacles. To this end, we use the setup depicted in Figure 5. First, we ensure that the line-of-sight path is blocked, and thus the docking station and the laptop can only communicate via reflections. Figure 20 validates this—the angular energy profile does not include any lobe

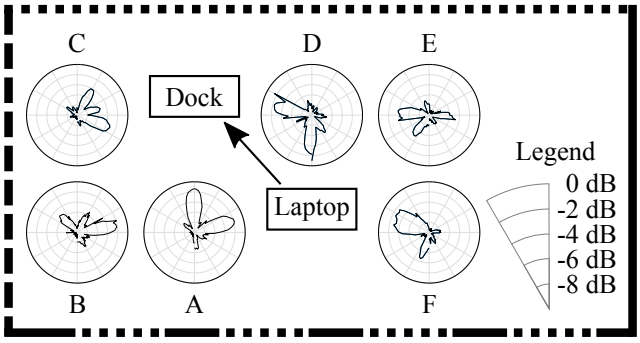

Figure 18: Reflections for Dell D5000.

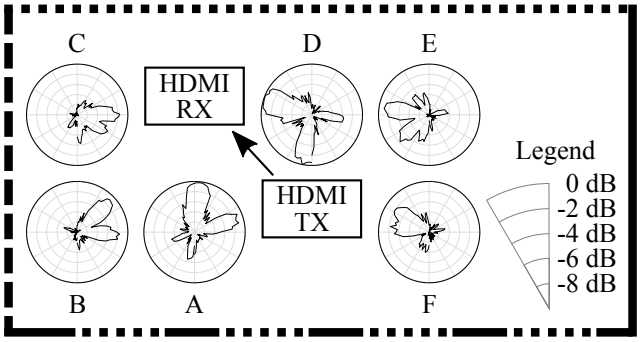

Figure 19: Reflections for DVDO Air-3c WiHD.

on the line-of-sight. Second, we use Iperf to measure the achievable throughput in this setup. We obtain 550 Mbps (±18 Mbps with 95% confidence) which is more than half of what we measure on line-of-sight links.

We show that commercial 60 GHz devices can achieve significant data rates on links with evidenced no line-of-sight component. Related work [14] shows similar findings but lacks validation via an angular energy profile.

4.4 Interference

In this section, we analyze the cross platform interference between the WiGig compliant Dell D5000 docking solution and the WiHD system. Both systems are forced to operate on the same channel, leading to imperfect channel usage coordination and interference. While the directionality of 60 GHz communication is supposed to severely limit interference we analyze two aspects of electronically steered indoor systems that can break this assumption. First, interference caused by the severe side lobes identified in Section 4.2 is analyzed by a setup with WiGig and WiHD devices operating in parallel. Second, we investigate the effect that can be caused by strong reflections as described in Section 4.3. To this aim, a combined setup of WiGig and WiHD devices is used, where the direct path between the two device classes is shielded. The measurement setups for both experiments are described in Section 3.2. We begin this section with the description of frame level effects observed for the interfering links which are the same for both setups. Then, details on the impact of link performance are given.

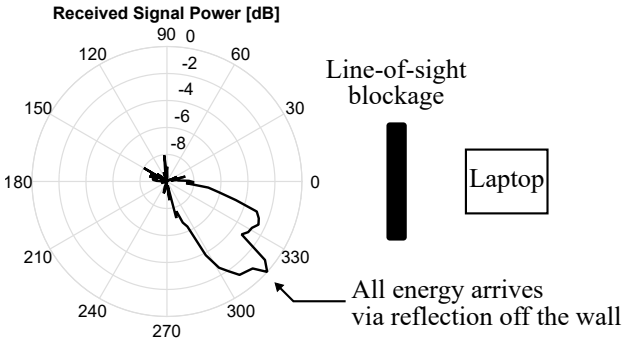

Figure 20: Angular energy profile at the docking station with link blockage (c.f. Figure 5).

Effects observed in frame level analysis. From a frame level analysis of the traffic flow between two interfering links, which follow different communication standards, we distinguish the following four different cases. First, data transmission of one system may occur during an idle period of the other system. In this case, there is a minor impact from the beacon frames transmitted by the interfering system, but we do not observe frame retransmissions or increased link utilization. Second, due to highly directional beam patterns, data streams may coexist without provoking retransmissions on the Dell D5000 link. Third, when links are close by, the D5000 shows enlarged data transmission gaps that are occupied by frames of the WiHD system. We assume this to be caused by a carrier sensing feature integrated in the Dell D5000. The same effect was found when two docking station links coexist. Finally, for close by links and overlapping transmissions, the D5000 shows missing acknowledgments and delays in the data frame flow. This indicates frame loss and retransmissions. In the latter two cases we also observe increased link utilization.

Figure 21 shows an example where both systems operate in parallel. Here, a typical D5000 data frame flow is interrupted by frames from the WiHD system. In particular, we observe collisions between 0.25 and 0.35 ms (first enlarged interval in Figure 21). The elevated noise floor indicates the presence of a weakly received WiHD frame, while at the same time D5000 data frames are transmitted. As the acknowledgments for these frames are missing, it is very likely that the three frames are retransmissions due to corrupted packet reception. Further, between 0.76 and 0.95 ms a dense series of WiHD data frames can be found (second enlarged interval in Figure 21). This series interrupts the usual D5000 data flow and does not suffer interference from the D5000 for a substantial time period. We attribute this behavior to the aforementioned carrier sensing of the D5000.

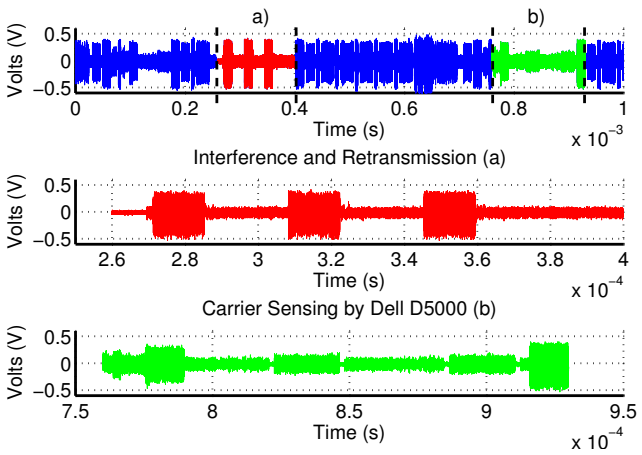

Figure 21: Inter system interference effects.

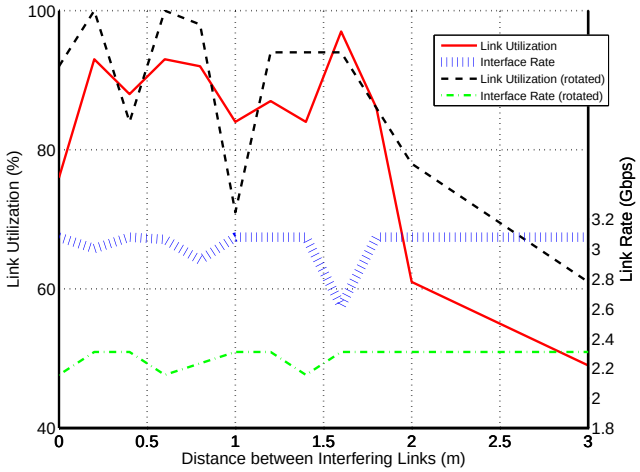

Figure 22: Side lobe interference impact.

Side Lobe Interference Impact. We now discuss the performance impact observed from side lobes for links in a parallel setup (compare Section 3.2), suffering from inter-system interference. The impact is evaluated in terms of observed link utilization, time for transmission of a file on the Dell 5000 system and the link rate reported by the D5000 WiGig driver application.

Figure 22 depicts the results for two setups: 1) an aligned D5000 link interfering with the WiHD system and 2) the same setup with the docking station misaligned by 70 degrees (denoted by 'rotated'). In the second setup, the docking station is beam-forming towards the outer limit of its serviceable transmission area and beam-forming performance is significantly worse as shown in Section 4.2. When comparing link utilization percentages, we find them to be significantly increased in both interference scenarios. We measure the interference free link utilization to be 38% and 42% in the aligned and rotated setup, respectively. Thus, we find a maximum link utilization increase of 62% and 58% for the two interference scenarios, which is significantly higher than the link utilization of the WiHD link alone, that we found to be 46%. The additional increase results from the frame collisions and retransmissions as described earlier in this section.

Even though we use two parallel Dell D5000 docking station links, the link utilization never saturates the channel. Thus, the measured transmission time stayed approximately constant despite retransmissions and carrier sensing induced delays. Therefore, we rely on the link utilization to asses the impact of interference. For higher network densities that saturate the channel and/or higher rate requirements of the wireless applications, interference is expected to have a significant impact on the throughput rate.

The difference of link utilization over the measured interference distances reveals a high interference regime for distances of up to two meters. When further increasing the distance of the second link, utilization reduces but only reaches interference free levels at distances beyond 5 meters. In the high interference regime, link utilization in the misaligned docking station setup is higher by around 10% compared to the aligned setup. At some measurement locations it reaches values of up to 100% and also shows a strongly varying pattern. For the aligned link we find a strong utilization increase to 97% at an interferer distance of 1.6 meters. We conjecture that this behavior is due to the side lobes that we observe for the data transmission antenna patterns of the D5000 link (compare Section 4.2). The fluctuating link utilization in the high interference regime for the misaligned link correlates well with its measured beam pattern that shows many strong side lobes. Unfortunately, we can not directly compare measured side lobes to the interference impact as it is not possible to measure receive antenna patterns. Also, since we cannot influence the selection of antenna patterns, it is not possible to ensure that the docking station uses the same pattern for both measurements.

From the reported link rates it can be clearly seen that the misaligned link performs worse due to the reduced beamforming capability at the limit of the antenna arrays transmission area, as explained in Section 4.2. Further, in the high interference regime below two meters link distance, an inverse correlation between link rate and link utilization is found. We assume the docking station link to adjust the link rate according to SINR measurements and packet loss statistics, thus the rate decreases under high link utilization that leads to an increase in collisions.

We find significant impact of inter-system interference on link utilization, especially when interferers with wide antenna patterns are as close as two meters. However, as current millimeter wave links are far from saturating the wireless link, there is little impact on the overall throughput achieved by the end systems. As rate

requirements and number of communicating devices increase, we expect to see a significant impact on throughput. We further find increased interference for antenna arrays focusing their beam close to the transmission area boundaries since patterns are less directional. The interference that we observe correlates well with the strong side lobes of the antenna patterns in Section 4.2.

Reflection Interference Impact. In this section we discuss TCP throughput measurements for a setup of WiGig and WiHD devices suffering inter-system interference via reflected paths. To this aim, we use a setup with a strong reflector. We shield the line-of-sight path between the links to protect from direct path and side lobe interference. The setup is described in Section 3.2.

The Iperf server used a 250 KByte TCP window and was configured to fully load the underlying Ethernet link, which was tunneled over the 60 GHz wireless link. While the WiGig tunneling managed to provide full gigabit speed for the Ethernet link, we found that it almost completely saturated the link. Most probably, this is because the D5000 system tries to minimize the delay of the Ethernet traffic. That is, instead of aggregating data to reduce the medium usage, the transmitter sends a larger number of packets, as discussed in Section 4.1. Because of this high medium usage, we expect the TCP link to be very sensitive to interference effects. Figure 23 shows the Iperf TCP throughput results for our reflection measurement. We observe that the TCP throughput increases significantly after about 90 seconds, which is when we power off the WiHD link. The performance degradation due to the WiHD reflection is about 200 mbps compared to the interference-free transmission. The strongest throughput loss occurs about 20 seconds after the start of the measurement—at that point, the throughput drops by almost 300 mbps. Further, we observe that the throughput fluctuates strongly for the case with interference. Most probably, these variations result from attempts of the D5000 to adapt to the high interference by switching among MCS levels.

When analyzing the effect of reflections on 60 *GHz communication, we find that, apart from an increase of the coverage area, also interference increases. For an isolated experiment setup with direct path blockage between links we find a severe impact on TCP throughput due to inter-system interference. The average throughput reduction was about* 20%*, and reached up to* 33%*.*

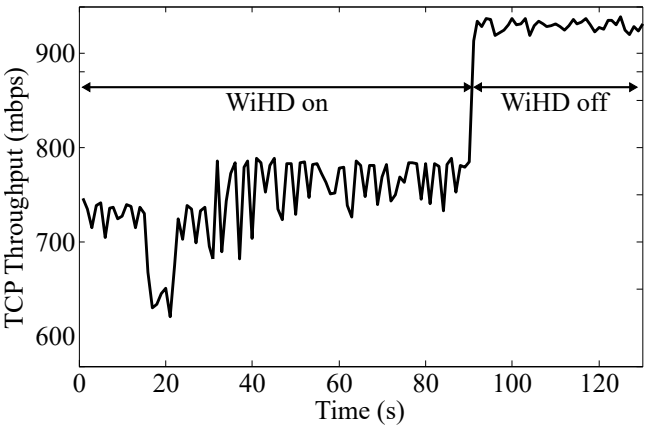

Figure 23: Reflection interference impact.

5. DISCUSSION

Analyzing commercial 60 GHz devices with the VubIQ system allows us to get new fundamental insights. This methodology makes our results stand apart from related work. In the following, we discuss these insights and derive design principles for 60 GHz practitioners.

Antenna patterns. We observe that the antenna pattern of consumer-grade 60 GHz devices not only exhibits significant side lobes due to its cost-effective design but also significantly depends on the specific location of the antenna array on the device. This hinders any assumptions regarding channel access at the MAC layer—in scenarios where devices with certain beam patterns do not interfere, others may cause collisions. As a design principle, we derive that 60 GHz networks should implement multiple MAC behaviors and choose the one which is most suitable for the beam patterns of the individual devices in the network.

Reflections. Our measurements show that 60 GHz signals may cause interference even after reflecting twice off walls. As a result, MAC layer designs which exploit the sparsity of 60 GHz signals to increase spatial reuse may incur unexpected collisions. Such designs are often based on geometric principles, that is, the beam pattern and range of a node define its area of interference. As a design principle, we derive that such protocols should extend this geometric approach to include up to two signal reflections off walls or obstacles if possible.

Aggregation. Our frame-level analysis reveals that 802.11ad aggregation provides large throughput gains at much smaller timescales than legacy systems. For instance, while 802.11ac achieves a 2× gain with a frame length of 8 ms (c.f. Table 1 in [19]), 802.11ad achieves a 5.4× gain by aggregating only up to 25 μs due to its very high data rates. Hence, the impact of aggregation on delay is much smaller for 802.11ad, while reducing dramatically channel usage time. As a design principle, we derive that the frame length should not only depend on the desired throughput and delay, but also on how many nodes share the medium. If many nodes share it due to, e.g., wide beam patterns, a higher aggregation level helps to provide channel time for all nodes.

Range. We show that, even in the same setup, the range of 60 GHz networks often varies significantly between experiments (c.f. Figure 13). This may be due to, e.g., different atmospheric conditions on different days. As a design principle, we derive that devices may need to adjust their transmit power to control interference even in quasi-static scenarios, such as homes.

6. CONCLUSION

We present an in-depth analysis of consumer-grade off-the-shelf 60 GHz systems. Our goal is to investigate the impact of the cost-effective designs of such devices. While these effects are often qualitatively well-known, we quantify them in order to provide a practical intuition on how important they are. This contributes crucial insights for the design of 60 GHz networking protocols. In particular, we investigate the impact of data aggregation, coding and modulation schemes (MCSs), beam patterns, reflections, and interference. We find that data aggregation yields throughput gains up to 5.4×. Further, MCS fluctuations may occur even in static environments due to beam realignments. Beamforming itself often results in strong side lobes due to the limitations of consumer-grade antennas. As a result, we observe significant interference in scenarios with two or more allegedly non-interfering 60 GHz links. We conclude that, while some common 60 GHz assumptions hold (e.g., data aggregation), others become critical for consumer-grade devices (e.g., impact of side lobes).

7. ACKNOWLEDGMENTS

This work is partially supported by the European Research Council grant ERC CoG 617721, the Ramon y Cajal grant from the Spanish Ministry of Economy and Competitiveness RYC-2012-10788, and the Madrid Regional Government through the TIGRE5-CM program (S2013/ICE-2919).

8. REFERENCES

[1] IEEE, "Wireless LAN Medium Access Control (MAC) and Physical Layer (PHY) Specifications Amendment 3: Enhancements for Very High Throughput in the 60 GHz Band," *IEEE Std 802.11ad-2012*, 2012.

[2] T. Nitsche, C. Cordeiro, A. Flores, E. Knightly, E. Perahia, and J. Widmer, "IEEE 802.11ad: directional 60 GHz communication for multi-Gigabit-per-second Wi-Fi [Invited Paper]," *IEEE Communications Magazine*, 2014.

[3] C. Cordeiro, D. Akhmetov, and M. Park, "Ieee 802.11Ad: Introduction and Performance Evaluation of the First Multi-gbps Wifi Technology," in *Proc. ACM mmCom*, 2010.

[4] N. Moraitis and P. Constantinou, "Indoor channel measurements and characterization at 60 GHz for wireless local area network applications," *IEEE Transactions on Antennas and Propagation*, vol. 52, no. 12, 2004.

[5] H. Xu, V. Kukshya, and T. S. Rappaport, "Spatial and temporal characteristics of 60-GHz indoor channels," *IEEE Journal on Selected Areas in Communications*, vol. 20, no. 3, 2002.

[6] H. Yang, P. Smulders, and M. Herben, "Frequency Selectivity of 60-GHz LOS and NLOS Indoor Radio Channels," in *Proc. 63rd IEEE VTC*, 2006.

[7] T. Zwick, T. Beukema, and H. Nam, "Wideband channel sounder with measurements and model for the 60 GHz indoor radio channel," *IEEE Transactions on Vehicular Technology*, vol. 54, no. 4, 2005.

[8] T. Manabe, Y. Miura, and T. Ihara, "Effects of antenna directivity and polarization on indoor multipath propagation characteristics at 60 GHz," *IEEE Journal on Selected Areas in Communications*, vol. 14, no. 3, 1996.

[9] K. Hosoya, N. Prasad, K. Ramachandran, N. Orihashi, S. Kishimoto, S. Rangarajan, and K. Maruhashi, "Multiple Sector ID Capture (MIDC): A Novel Beamforming Technique for 60-GHz Band Multi-Gbps WLAN/PAN Systems," *IEEE Transactions on Antennas and Propagation*, vol. 63, no. 1, 2015.

[10] A. Lamminen, J. Saily, and A. Vimpari, "60-GHz Patch Antennas and Arrays on LTCC With Embedded-Cavity Substrates," *IEEE Transactions on Antennas and Propagation*, 2008.

[11] X.-P. Chen, K. Wu, L. Han, and F. He, "Low-Cost High Gain Planar Antenna Array for 60-GHz Band Applications," *IEEE Transactions on Antennas and Propagation*, vol. 58, no. 6, 2010.

[12] S. B. Yeap, Z. N. Chen, and X. Qing, "Gain-Enhanced 60-GHz LTCC Antenna Array With Open Air Cavities," *IEEE Transactions on Antennas and Propagation*, vol. 59, no. 9, 2011.

[13] X. Tie, K. Ramachandran, and R. Mahindra, "On 60 ghz wireless link performance in indoor environments," in *Passive and Active Measurement*, ser. Lecture Notes in Computer Science, 2012, vol. 7192.

[14] Y. Zhu, Z. Zhang, Z. Marzi, C. Nelson, U. Madhow, B. Y. Zhao, and H. Zheng, "Demystifying 60GHz Outdoor Picocells," in *Proc. ACM Mobicom*, 2014.

[15] C. Hansen, "WiGiG: Multi-gigabit wireless communications in the 60 GHz band," *IEEE Wireless Communications*, vol. 18, no. 6, 2011.

[16] P. Schmulders, "Exploiting the 60 GHz Band for Local Wireless Multimedia Access: Prospects and Future Directions," *IEEE Communications Magazine*, vol. 40, no. 1, 2002.

[17] S. Sur, V. Venkateswaran, X. Zhang, and P. Ramanathan, "60 ghz indoor networking through flexible beams: A link-level profiling," in *Proc. ACM SIGMETRICS*, 2015.

[18] Vubiq. V60WGD03 60 GHz Waveguide Development System. [Online]. Available: http://www.pasternack.com/60-ghz-development-systems-category.aspx

[19] S. Byeon, K. Yoon, O. Lee, S. Choi, W. Cho, and S. Oh, "Mofa: Mobility-aware frame aggregation in wi-fi," in *Proc. ACM CoNEXT*, 2014.